Ocean-arcs as a hidden cooling mechanism during the early Paleozoic

Andrew Merdith[1,*], Maëlis Arnould[2], Lucy McGee[1], Alexandre Janin[3], Simon Williams[4], Stefan Loehr[1], Morgan Blades[1], Benjamin J. W. Mills[5]

[1] School of Physics, Chemistry and Earth Sciences, University of Adelaide, Australia

[2] Université Claude Bernard Lyon 1, École Normale Supérieure de Lyon, CNRS, Université Jean Monnet, LGL-TPE, UMR 5276, Villeurbanne, France

[3] Department of Earth and Environmental Sciences, Boston College, Chestnut Hill, MA, USA

[4] Institute for Marine and Antarctic Studies, University of Tasmania, Hobart, TAS, Australia

[5] School of Earth and Environment, University of Leeds, UK

*Corresponding author (Andrew.merdith@adelaide.edu.au)

Peer review status:
This is a non-peer-reviewed preprint submitted to EarthArXiv

Ocean-arcs as a hidden cooling mechanism during the early Paleozoic

Andrew Merdith[1], Maëlis Arnould[2], Lucy McGee[1], Alexandre Janin[3], Simon Williams[4], Stefan Loehr[1], Morgan Blades[1], Benjamin J. W. Mills[5]

[1] School of Physics, Chemistry and Earth Sciences, University of Adelaide, Australia

[2] Université Claude Bernard Lyon 1, École Normale Supérieure de Lyon, CNRS, Université Jean Monnet, LGL-TPE, UMR 5276, Villeurbanne, France

[3] Department of Earth and Environmental Sciences, Boston College, Chestnut Hill, MA, USA

[4] Institute for Marine and Antarctic Studies, University of Tasmania, Hobart, TAS, Australia

[5] School of Earth and Environment, University of Leeds, UK

ABSTRACT

The late Cambrian to end Ordovician is marked by a long-term climatic cooling, culminating with the short lived (<2 Ma) Hirnantian icehouse, before recovering to warmer climates. Increased silicate weathering during the Laurentian Taconic orogeny, driven by the accretion of ocean island arcs and obduction of ophiolites, has been invoked as a causal mechanism to help explain cooling. However, prior to their accretion or obduction through arc-continent collision, these will have occurred as a series of mafic–intermediate volcanic islands. At the present-day, oceanic island arcs located in equatorial regions contribute the highest silicate weathering flux globally. We demonstrate that the abundance and evolution of low latitude ocean arcs in the late Cambrian and Ordovician can help account for gradual cooling over this time. We extract estimates of ocean arc lengths from a full-plate reconstruction and, using constraints from the present day, parameterise their potential contribution to the silicate

weathering cycle within an Earth System model (*SCION)*. We show that ocean arc weathering induces a minimum cooling of 1–2°C, and up to 5–7°C in our preferred scenario and helps reconcile model strontium and osmium isotope records with geochemical proxy data. We conclude that the prevalence of ocean-arcs and associated delivery of mafic weathering material was an important contributor to silicate weathering at this time and could be an overlooked CO_2 drawdown mechanism throughout Earth history.

INTRODUCTION

The late Cambrian to Ordovician Earth (~500–445 Ma) was marked by growing biodiversity and cooling climate. The fossil record during this time reveals one of the most significant and sustained periods of biodiversification, with family and genus level taxa increasing 3–4 fold (Droser et al., 1996; Sepkoski, 1996; Servais et al., 2010). This increase in biodiversity has usually been explained by a cooling climate, where equatorial mean sea surface temperatures were proposed to fall from ~40°C in the late Cambrian towards modern day values of 25–30°C during the Ordovician enlarging the habitable range for organisms, (Trotter et al., 2008), before reaching their lowest point during the Hirnantian glaciation at ~445 Ma (Finnegan et al., 2011) (Fig. 1).

Potential causal mechanisms for global cooling during the Ordovician are varied, though the protracted nature of cooling is widely considered to require a continuous tectonic driver (Edwards et al., 2017; Marcilly et al., 2022). Hypotheses include: a decrease in solid-Earth degassing (McKenzie et al., 2016); an increased exposure of weatherable rocks around the tropics, particularly through ocean arc-continent sutures (Kump et al., 1999; Swanson-Hysell and Macdonald, 2017); evolution of land plants and beginning of the terrestrial organic carbon

pump (Lenton et al., 2012); an increase in marine organic carbon burial (Brenchley et al., 1994) and changes in paleogeography and sea level (Pohl et al., 2014). However, numerical models that largely include these processes fail to reconstruct the observed extent and timescale of cooling (Mills et al., 2021; Marcilly et al., 2022), suggesting that there could be a missing key component. The low-latitude weathering of oceanic island arcs (Swanson-Hysell and Macdonald, 2017), is one such mechanism that has not been examined in detail and the focus in this study.

WEATHERING OF OCEAN ARCS

Volcanic arcs, both continental and oceanic, are thought to exert a fundamental control on Earth's long-term climate (McKenzie et al., 2016). They are sites of carbon degassing from the solid-Earth to the atmosphere and generate large amounts of silicate-rich volcanic rocks, typically in landscapes defined by high elevation and relief, which in turn drive increased rainfall, erosion and weathering. Thus, in theory, they act as both source *and* sink with respect to the long-term carbon cycle (Lee et al., 2015).

Active ocean arcs are distributed across all latitudes of the globe at the present-day, where they are key, but often overlooked, contributors to chemical weathering (Allègre et al., 2010; Gaillardet et al., 2011b). In our analysis we focus on those arcs that fall within equatorial (±15°) regions where the intertropical convergence zone produces a tropical rain belt and denudation rates are highest. Measurements of chemical weathering fluxes for equatorial arcs (e.g. Philippines and Lesser Antilles) are amongst the highest observed on Earth (Gaillardet et al., 2011a), at 40 to 400 t/km^2/a, encompassing the weathering of both basaltic (mafic) and andesitic (intermediate) lithologies. In comparison, global analyses of river catchments suggest

an average flux of 10–24 t/km^2/a (Gaillardet et al., 1999; Hartmann et al., 2014) indicating that the weathering flux is highly bimodal, with the aforementioned tropical regions built on mafic–intermediate islands contributing an order of magnitude more silicate cations than the global average per unit area.

Estimating the lengths of Ordovician oceanic arcs

The influence of oceanic arcs on climate, especially in the pre-Pangea world, has not been considered in detail, partly because of how poorly they are preserved in the geological record in comparison to continental arcs, and also how difficult it is to restore them to their correct paleo-positions (Safonova et al., 2017). Full-plate reconstructions that restore ancient plate boundaries and tectonic plates in a self-consistent, continuous framework (Seton et al., 2023) offer a possible avenue to overcome this limitation. These models require a network of fully interconnected plate boundaries; thus they include both explicit oceanic arcs based on the geological record and implicit oceanic-arcs that are required by plate tectonic theory to accommodate for plate-motion (Domeier, 2018).

The Ordovician Period, occurring just after the final amalgamation of Gondwana, has an unusual global paleogeographic configuration, with all known continental lithosphere in the southern hemisphere, and the northern hemisphere being predominantly oceanic lithosphere (Fig. 2). Along the southern margin of Gondwana, the Terra Australis orogen developed as a long-lived and reasonably stable continental arc. However, at each of the western and eastern ends of this arc, and along the northern margin of Gondwana, subduction instead was expressed as a series of rifted ribbon terranes, leading to successive generations of oceans opening and closing, and the generation of many intraoceanic arcs (Table S2).

To isolate oceanic arcs we extracted subduction zones from the model of Merdith et al. (2021) (MER21), which incorporates modifications to the early Paleozoic model of Domeier (2018) (see Suppl. Material; Figs. S1–S5). For each subduction segment, we calculated its distance to the nearest continent (Fig. 2). Segments beyond a defined threshold were classified as oceanic arcs, whereas those within the threshold were classified as peri-continental. Using a 400 km threshold (mean plus standard deviation trench-continental arc distance along present-day subduction zones (Zahirovic et al., 2022)), we classify ~22,500 km (35%) of present-day subduction as oceanic (Fig. 2a), compared with ~40,000 km (50%) at the Cambrian–Ordovician boundary and ~28,000 km (35%) by the end Ordovician (Fig. 3).

Ocean arcs as an extra source of silicate weathering?

To test our hypothesis that oceanic arcs can help drive net global cooling, we use the *SCION* model (Mills et al., 2021; Merdith et al., 2025). *SCION* calculates the global long-term carbon, oxygen, sulfur, phosphorous and nitrogen cycles using spatially explicit representations of hydrology, climate and topography. The *SCION* model does not explicitly include ocean-arc terranes, and we consider the unaltered model as our 'default' model. We devised a way to estimate their contributions to the silicate weathering cycle and consider three scenarios. Our first scenario assumes that the 'active' (i.e. subducting) length of ocean arcs at each time-step exerts a proportional control over the extent of weatherable (ocean arc) features at that time. Our second and third scenarios follow from this, and assume an extended island lifespan (5 and 10 Ma respectively) between the formation of a volcanic island and its erosion to sea level, potentially due to subduction shutoff, arc migration, or the development of new melting zones

in the overriding plate further extending the duration of island-arc weathering (Table S2, Fig S6).

In all scenarios we consider three additional parameters relating to the reconstructed lengths of ocean arcs, to calculate their total contribution to chemical weathering. Firstly, we extracted lengths of oceanic arcs from the MER21 model, binned at 1 Ma intervals and 5° latitude bands, and then restricted the data to within ±~15° of the equator. The first two parameters we consider are the proportion of the along strike arc that consists of subaerial islands (α), and the width (ω) of those islands. Multiplying the length of the oceanic arcs by these two parameters gives an estimate of the area of subaerial, basaltic–andesitic islands formed through ocean-ocean convergence. A final parameter, the silicate weathering flux per km^2 (ε), is used to quantify the total silicate weathering flux from these islands (τ). In all three scenarios described above (0, 5 and 10 Ma lifespan of islands) we run a series of models across a range of parameter (α, ω, ε) values, constraining their ranges with present-day Earth measurements. These are summarised, and the calculated chemical weathering fluxes of each scenario are provided in Table S2 and the Supp. Data. We do not alter degassing, paleogeography, or the previously established weatherability of continental and obducted arcs in the *SCION* model (Merdith et al., 2025). Since the plant evolution functions are only relevant from 450 Ma to present, they are not considered in this work. Finally, to better evaluate our models, given the uncertainty in both the extents and locations of ocean arcs, we also implemented a radiogenic Osmium (Os) isotopic model after Sproson et al. (2022). Figure 4 shows the SCION results from our preferred scenario (the 10 Ma lifespan, which better reflects the duration of islands, see Figs. S7, S8 for the 0 and 5 Ma lifespan results).

OCEAN ARCS AS A COOLING MECHANISM

Our default model, which excludes additional weathering contributions from oceanic arcs (black dashed lines Fig. 4), produces a reasonably warm, but not fully ice free, Cambrian and Ordovician world. In this case, the early Paleozoic Earth maintains a global average surface temperature (GAST) of 21–23°C. The different scenarios highlighted above induce moderate (2–4°C) to substantial (4–7°C) cooling, depending on the exact parameters. Our preferred scenario (10 Ma lifespan), results in a ~7°C cooling from the late Cambrian (~23°C GAST at 500 Ma) to Early Ordovician (~17°C GAST at 480 Ma), followed by a partial recovery to ~19°C GAST during the Middle Ordovician. A renewed cooling trend begins in the Late Ordovician, with temperatures cooling from ~20°C to ~17°C during the Hirnantian Glaciation. Incorporating volcanic-phosphorus–induced cooling as in previous models (Longman et al., 2021) produces an additional spike, lowering GAST to ~14 °C in the Hirnantian, before a rapid recovery to ~23 °C in the Silurian (~435 Ma). GAST recovers quickly in the Silurian, returning to ~23° by ~435 Ma. Overall, these trends are replicated for all different parameter combinations, although more conservative estimates of ocean-arc weathering (i.e. silicate fluxes of 40 t/km^2/a) results in only 1–2°C of cooling over the Early Ordovician. To reach a Hirnantian GAST of ~18°C, consistent with the assumed threshold for ice house conditions (Scotese et al., 2021), a minimum weathering contribution of 400 t per km of arc length is required.

The available Os and Sr proxy data through the early Paleozoic both show a similar decreasing trend across the Ordovician (Fig. 4). The modelled results of both cycles for the default run (no contribution of ocean arcs) produce a functionally flat line for the model duration. In comparison, when we include the unradiogenic contributions from ocean arc weathering both our modelled Os and Sr align more closely with the proxy data. During the Early Cambrian,

both our modelled Os and Sr seawater curves are in much better, but not full, agreement with the proxy data. After 500 Ma, the onset of subduction preserved in the Sunnhordland and Köli arcs outboard of north-eastern Laurentia drives a decrease in the modelled isotopic ratios of both elements. The closure of these arcs around 480 Ma stalls our modelled cooling alongside the decrease in Os and Sr ratios. The re-onset of cooling at 460 Ma is driven principally by the northward motion of both Siberia and Baltica (Fig. 2), and the resulting movement of three oceanic arcs into the tropical belt: the Guberlya Tagil arc on the (reconstructed) southern margin of Siberia, an inferred oceanic arc outboard of Kara and Baltica, accommodating the northward drift of the two, and the ocean arcs preserved off the south of the Tarim craton in the Qaidam-Qilian region (Fig. 2). At 440 Ma our model begins warming and our modelled Os and Sr seawater compositions begin increasing. This move towards more radiogenic values in the Sr data is supported by the proxy record, though there are no Silurian aged proxy data for Os in our compilation. For both elements, this change is driven in the model at ca. 440 Ma by the equatorial ocean arcs colliding and the cessation of subduction.

The primary cause of Ordovician cooling is enigmatic. Swanson Hysell and MacDonald (2017) have suggested that the emplacement of ophiolitic bearing sutures during this time could have driven global cooling. A key limitation of this hypothesis is that ophiolites, once emplaced, contribute finitely to chemical weathering, before they are either fully weathered, or buried. Instead, we test another idea, also hypothesised by Swanson Hysell and MacDonald (2017), that active ocean island arcs could also have contributed to cooling over their lifespan. Unlike ophiolites, arcs overcome the finite-weathering limitation, as, provided there is an active arc, volcanism can continually replenish silicate cations, and in all our tested scenarios this process produces a net cooling effect over the Ordovician. There are other times where a predominance of tropical ocean-arcs have been noted, during the late Tonian and Cryogenian where extensive

juvenile terranes have been documented through the Arabian-Nubian Shield (Hargrove et al., 2006) and in eastern Dronning Maud Land (Jacobs et al., 2017), and also possibly during the Mesozoic, where intra-ocean subduction spanned the Tethyan and Pacific Oceans (Domeier et al., 2017). Consequently, the prevalence of ocean arcs could help explain previous icehouses or cool periods in Earth history.

CONCLUSIONS

Our modelling of ocean-arc contributions to silicate weathering during the early Paleozoic demonstrates that they could help drive cooling over this time. By using present-day weathering rates from island-arcs and estimates of their varying lengths in the geological past from full-plate models, we were able to incorporate their contribution to tropical weathering in a climate-carbon model. Our resulting model shows a much stronger fit to Sr and Os isotope records than the default model, indicating that extra weathering from ocean arcs could be a plausible source of silicate cations and unradiogenic strontium and osmium to the oceans at this time. Our analysis shows that up to 5 °C of cooling over the Ordovician can be induced from weathering of tropical ocean-arcs, potentially helping explain the changes in climate over this time, and demonstrating a mechanism that may be important during other periods of Earth's history.

ACKNOWLEDGEMENTS

Funding for this work includes ARC DECRA DE230101642 and MSCA-IF, 893615 (ASM), UKRI project EP/Y008790/1(BJWM). UKRI project NE/X011208/1 (ASM and BJWM).

FIGURE CAPTIONS

Figure 1: Earth's global average surface temperature (GAST) and iceline proxy data. Green and orange curves are temperature proxies from Scotese et al. (2021) and Judd et al. (2024), respectively, represented by $\mu \pm 1\sigma$ envelope. Blue line is iceline from Van der Meer et al. (2022). C, Cambrian; O, Ordovician; h, Hirnantian; S, Silurian; D, Devonian.

Figure 2: Reconstructed maps from MER21 with subduction zones outlined, coloured by the distance between them and the nearest (modelled) piece of continental crust (represented by the light green polygons). Equatorial range used in our analysis is highlighted. MQ, Macquarie arc, SK, Sunnhordland and Köli arcs; LB, Lushs Bight arc; AS, Alta-Sayan arcs; SSEU, Stepnyak, Selety, Erementau, Urumbai arcs; DH, Dunhuang-Hanshan arc; GTg, Guberlya Tagil arc; KQQ, Kunlun-Qaidam-Qinlin arcs. Arcs '?1–5' are required by the model to account for plate motion but have limited direct evidence in the geological record, see Table S1.

Figure 3: Summary of ocean arcs in our model. (a) Overall length of ocean arcs vs. time using different proximity parameters. For our analysis we pick a 400 km threshold to distinguish oceanic vs peri-continental arcs. (b) Heatmap of ocean arc length vs latitude using the 400 km threshold over the Phanerozoic. Red lines show equatorial (±15°) regions.

Figure 4: Preferred model results assuming a 10 Ma life span of ocean arc islands with proxy data. Default model run (i.e. no contribution from ocean arcs) is shown as the black dashed line in each respective panel. (a) global average surface temperature. (b) modelled $^{187/188}$Os of seawater. (c) modelled iceline results. (d) modelled $^{87/86}$Sr of seawater. Proxies from Figure 1 are depicted in blue.

Supplemental Material. Supplementary material includes discussion around: paleogeographic uncertainty, including alternative SCION runs with the Domeier (2018) model; present-day constraints on islands at oceanic-arcs, alterations to the SCION model, model outputs, and model code to recreate results. Please visit https://zenodo.org/records/17345053 to access the model code, and contact editing@geosociety.org with any questions.

REFERENCES CITED

Allègre, C.J., Louvat, P., Gaillardet, J., Meynadier, L., Rad, S., and Capmas, F., 2010, The fundamental role of island arc weathering in the oceanic Sr isotope budget: Earth and planetary science letters, v. 292, p. 51–56.

Brenchley, P.J., Marshall, J.D., Carden, G.A.F., Robertson, D.B.R., Long, D.G.F., Meidla, T., Hints, L., and Anderson, T.F., 1994, Bathymetric and isotopic evidence for a short-lived Late Ordovician glaciation in a greenhouse period: Geology, v. 22, p. 295–298.

Domeier, M., 2018, Early Paleozoic tectonics of Asia: Towards a full-plate model: Geoscience Frontiers, v. 9, p. 789–862.

Domeier, M., Shephard, G.E., Jakob, J., Gaina, C., Doubrovine, P.V., and Torsvik, T.H., 2017, Intraoceanic subduction spanned the Pacific in the Late Cretaceous-Paleocene: Science advances, v. 3, doi:10.1126/sciadv.aao2303.

Droser, M.L., Fortey, R.A., and Li, X., 1996, The Ordovician Radiation: American Scientist, v. 84, p. 122–131.

Edwards, C., Saltzman, M., Royer, D., and Fike, D., 2017, Oxygenation as a driver of the Great Ordovician Biodiversification Event: Nature geoscience, v. 10, p. 925–929.

Finnegan, S., Bergmann, K., Eiler, J.M., Jones, D.S., Fike, D.A., Eisenman, I., Hughes, N.C., Tripati, A.K., and Fischer, W.W., 2011, The Magnitude and Duration of Late Ordovician–Early Silurian Glaciation: Science, v. 331, p. 903–906.

Gaillardet, J., Dupré, B., Louvat, P., and Allègre, C.J., 1999, Global silicate weathering and CO2 consumption rates deduced from the chemistry of large rivers: Chemical geology, v. 159, p. 3–30.

Gaillardet, J., Louvat, P., and Lajeunesse, E., 2011a, Rivers from Volcanic Island Arcs: The subduction weathering factory: Applied geochemistry: journal of the International Association of Geochemistry and Cosmochemistry, v. 26, p. S350–S353.

Gaillardet, J., Rad, S., Rive, K., Louvat, P., Gorge, C., Allegre, C.J., and Lajeunesse, E., 2011b, Orography-driven chemical denudation in the Lesser Antilles: Evidence for a new feed-back mechanism stabilizing atmospheric CO2: American journal of science, v. 311, p. 851–894.

Hargrove, U.S., Stern, R.J., Kimura, J.-I., Manton, W.I., and Johnson, P.R., 2006, How juvenile is the Arabian–Nubian Shield? Evidence from Nd isotopes and pre-Neoproterozoic inherited zircon in the Bi'r Umq suture zone, Saudi Arabia: Earth and planetary science letters, v. 252, p. 308–326.

Hartmann, J., Moosdorf, N., Lauerwald, R., Hinderer, M., and West, A.J., 2014, Global chemical weathering and associated P-release — The role of lithology, temperature and soil properties: Chemical geology, v. 363, p. 145–163.

294 Jacobs, J., Opås, B., Elburg, M.A., Läufer, A., Estrada, S., Ksienzyk, A.K., Damaske, D., and
295 Hofmann, M., 2017, Cryptic sub-ice geology revealed by a U-Pb zircon study of glacial
296 till in Dronning Maud Land, East Antarctica: Precambrian research, v. 294, p. 1–14.

297 Judd, E.J., Tierney, J.E., Lunt, D.J., Montañez, I.P., Huber, B.T., Wing, S.L., and Valdes, P.J.,
298 2024, A 485-million-year history of Earth's surface temperature: Science (New York,
299 N.Y.), v. 385, p. eadk3705.

300 Kump, L.R., Arthur, M.A., Patzkowsky, M.E., Gibbs, M.T., Pinkus, D.S., and Sheehan, P.M.,
301 1999, A weathering hypothesis for glaciation at high atmospheric pCO2 during the Late
302 Ordovician: Palaeogeography, palaeoclimatology, palaeoecology, v. 152, p. 173–187.

303 Lee, C.-T.A., Thurner, S., Paterson, S., and Cao, W., 2015, The rise and fall of continental arcs:
304 Interplays between magmatism, uplift, weathering, and climate: Earth and planetary
305 science letters, v. 425, p. 105–119.

306 Lenton, T.M., Crouch, M., Johnson, M., Pires, N., and Dolan, L., 2012, First plants cooled the
307 Ordovician: Nature geoscience, v. 5, p. 86–89.

308 Longman, J., Mills, B.J.W., Manners, H.R., Gernon, T.M., and Palmer, M.R., 2021, Late
309 Ordovician climate change and extinctions driven by elevated volcanic nutrient supply:
310 Nature geoscience, v. 14, p. 924–929.

311 Marcilly, C.M., Maffre, P., Le Hir, G., Pohl, A., Fluteau, F., Goddéris, Y., Donnadieu, Y., H.
312 Heimdal, T., and Torsvik, T.H., 2022, Understanding the early Paleozoic carbon cycle
313 balance and climate change from modelling: Earth and planetary science letters, v. 594,
314 p. 117717.

McKenzie, N.R., Horton, B.K., Loomis, S.E., Stockli, D.F., Planavsky, N.J., and Lee, C.-T.A., 2016, Continental arc volcanism as the principal driver of icehouse-greenhouse variability: Science, v. 352, p. 444–447.

van der Meer, D.G., Scotese, C.R., Mills, B.J.W., Sluijs, A., van den Berg van Saparoea, A.-P., and van de Weg, R.M.B., 2022, Long-term Phanerozoic global mean sea level: Insights from strontium isotope variations and estimates of continental glaciation: Gondwana Research, v. 111, p. 103–121.

Merdith, A.S. et al., 2021, Extending full-plate tectonic models into deep time: Linking the Neoproterozoic and the Phanerozoic: Earth-Science Reviews, v. 214, p. 103477.

Merdith, A.S., Gernon, T.M., Maffre, P., Donnadieu, Y., Goddéris, Y., Longman, J., Müller, R.D., and Mills, B.J.W., 2025, Phanerozoic icehouse climates as the result of multiple solid-Earth cooling mechanisms: Science advances, v. 11, p. eadm9798.

Mills, B.J.W., Donnadieu, Y., and Goddéris, Y., 2021, Spatial continuous integration of Phanerozoic global biogeochemistry and climate: Gondwana Research, doi:10.1016/j.gr.2021.02.011.

Pohl, A., Donnadieu, Y., Le, H.G., Buoncristiani, J.F., and Vennin, E., 2014, Effect of the Ordovician paleogeography on the (in) stability of the climate: Climate of the Past, v. 10, p. 2053–2066.

Safonova, I., Kotlyarov, A., Krivonogov, S., and Xiao, W., 2017, Intra-oceanic arcs of the Paleo-Asian ocean: Gondwana research: international geoscience journal, v. 50, p. 167–194.

Scotese, C.R., Song, H., Mills, B.J.W., and van der Meer, D.G., 2021, Phanerozoic paleotemperatures: The earth's changing climate during the last 540 million years: Earth-science reviews, v. 215, p. 103503.

Sepkoski, J.J., Jr, 1996, Patterns of Phanerozoic extinction: A perspective from global data bases, *in* Global Events and Event Stratigraphy in the Phanerozoic, Berlin, Heidelberg, Springer Berlin Heidelberg, p. 35–51.

Servais, T., Owen, A.W., Harper, D.A.T., Kröger, B., and Munnecke, A., 2010, The Great Ordovician Biodiversification Event (GOBE): The palaeoecological dimension: Palaeogeography, palaeoclimatology, palaeoecology, v. 294, p. 99–119.

Seton, M., Williams, S.E., Domeier, M., Collins, A.S., and Sigloch, K., 2023, Deconstructing plate tectonic reconstructions: Nature Reviews Earth & Environment, p. 1–20.

Sproson, A.D. et al., 2022, Osmium and lithium isotope evidence for weathering feedbacks linked to orbitally paced organic carbon burial and Silurian glaciations: Earth and planetary science letters, v. 577, p. 117260.

Swanson-Hysell, N.L., and Macdonald, F.A., 2017, Tropical weathering of the Taconic orogeny as a driver for Ordovician cooling: Geology, v. 45, p. 719–722.

Trotter, J.A., Williams, I.S., Barnes, C.R., Lécuyer, C., and Nicoll, R.S., 2008, Did cooling oceans trigger Ordovician biodiversification? Evidence from conodont thermometry: Science (New York, N.Y.), v. 321, p. 550–554.

Zahirovic, S., Eleish, A., Doss, S., Pall, J., Cannon, J., Pistone, M., Tetley, M.G., Young, A., and Fox, P., 2022, Subduction and carbonate platform interactions: Geoscience data journal, doi:10.1002/gdj3.146.

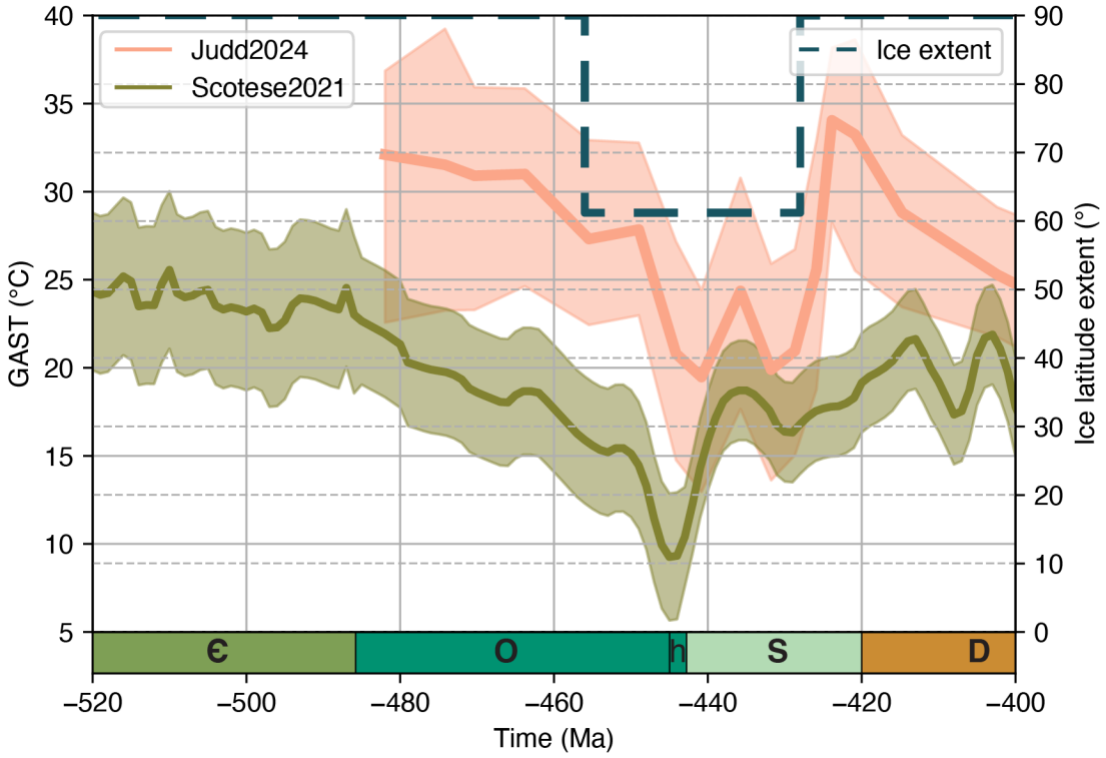

Figure 1: Earth's global average surface temperature (GAST) and iceline proxy data. Green and orange curves are temperature proxies from Scotese et al. (2021) and Judd et al. (2024), respectively, represented by a mean and a 1 standard deviation envelope. Blue line is iceline from Van der Meer et al. (2022). C, Cambrian; O, Ordovician; h, Hirnantian; S, Silurian; D, Devonian.

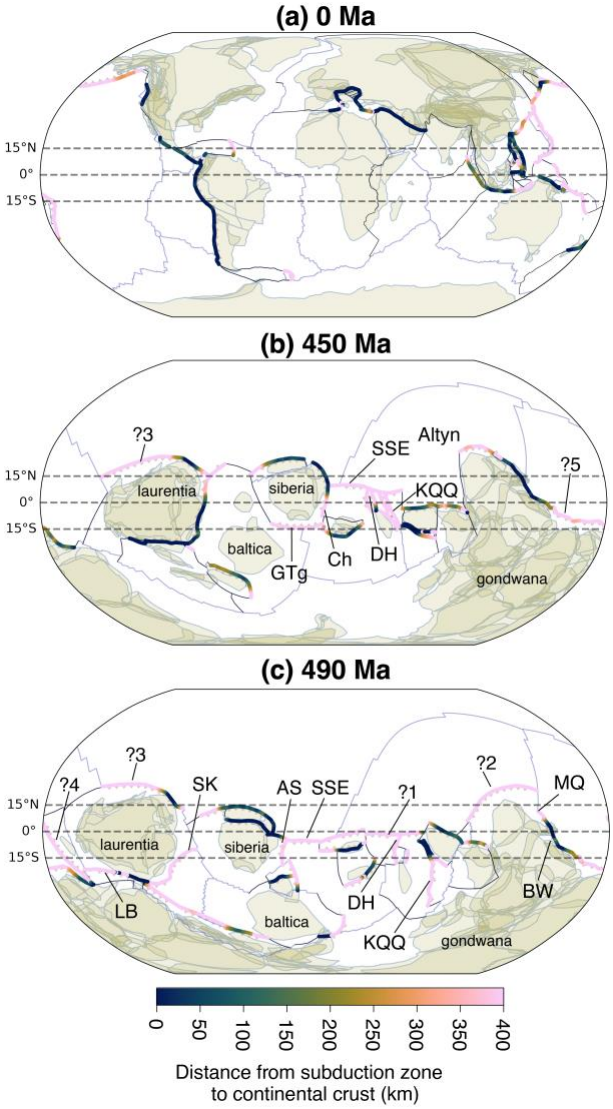

Figure 2: Reconstructed maps from MER21 with subduction zones outlined, coloured by the distance between them and the nearest (modelled) piece of continental crust (represented by the light green polygons). Equatorial range used in our analysis is highlighted. BW, Bowers arc; MQ, Macquarie arc, SK, Sunnhordland and Köli arcs; LB, Lushs Bight arc; AS, Alta-Sayan arcs (Kuznetsk-Alatua, north Sayan, Lake Khamsara, Chingiz); SSEU, Stepnyak, Selety, Erementau, Urumbai arcs; DH, Dunhuang-Hanshan arc; GTg, Guberlya Tagil arc; KQQ, Kunlun-Qaidam-Qinlin arcs. Arcs '?1–5' are required by the model to account for plate motion but have limited direct evidence in the geological record.

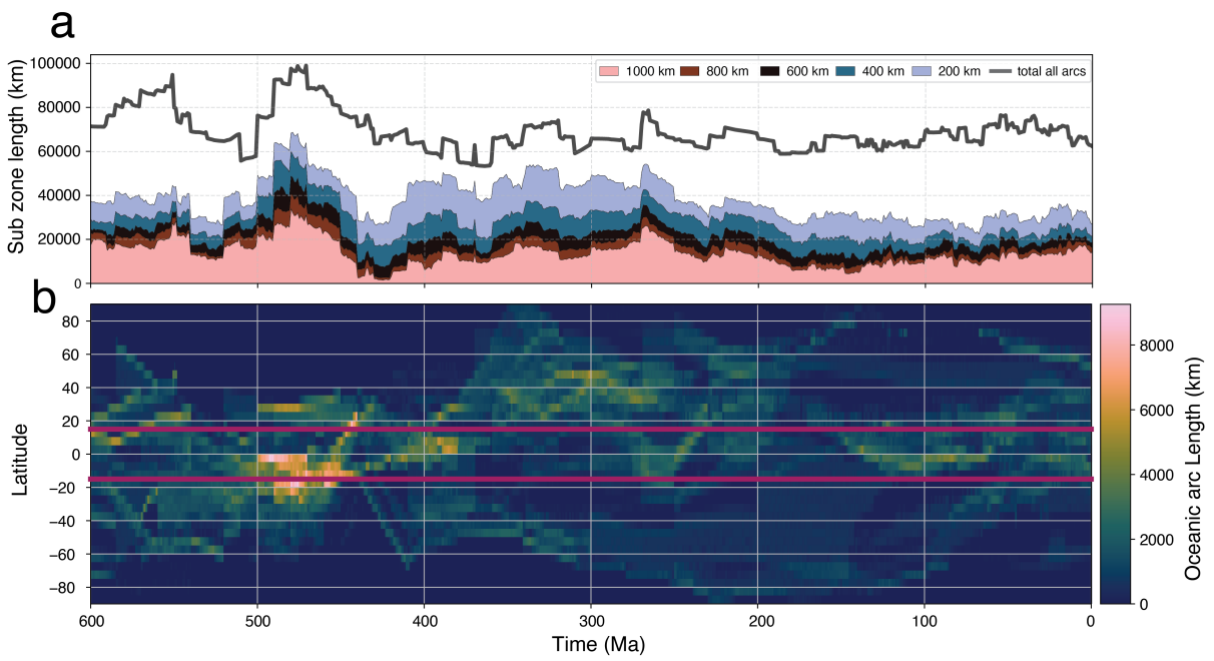

Figure 3: Summary of ocean arcs in our model. (a) Overall length of ocean arcs vs. time using different proximity parameters. For our analysis we pick a 400 km threshold to distinguish oceanic vs peri-continental arcs. (b) Heatmap of ocean arc length vs latitude using the 400 km threshold over the Phanerozoic. Red lines show equatorial (±15°) regions.

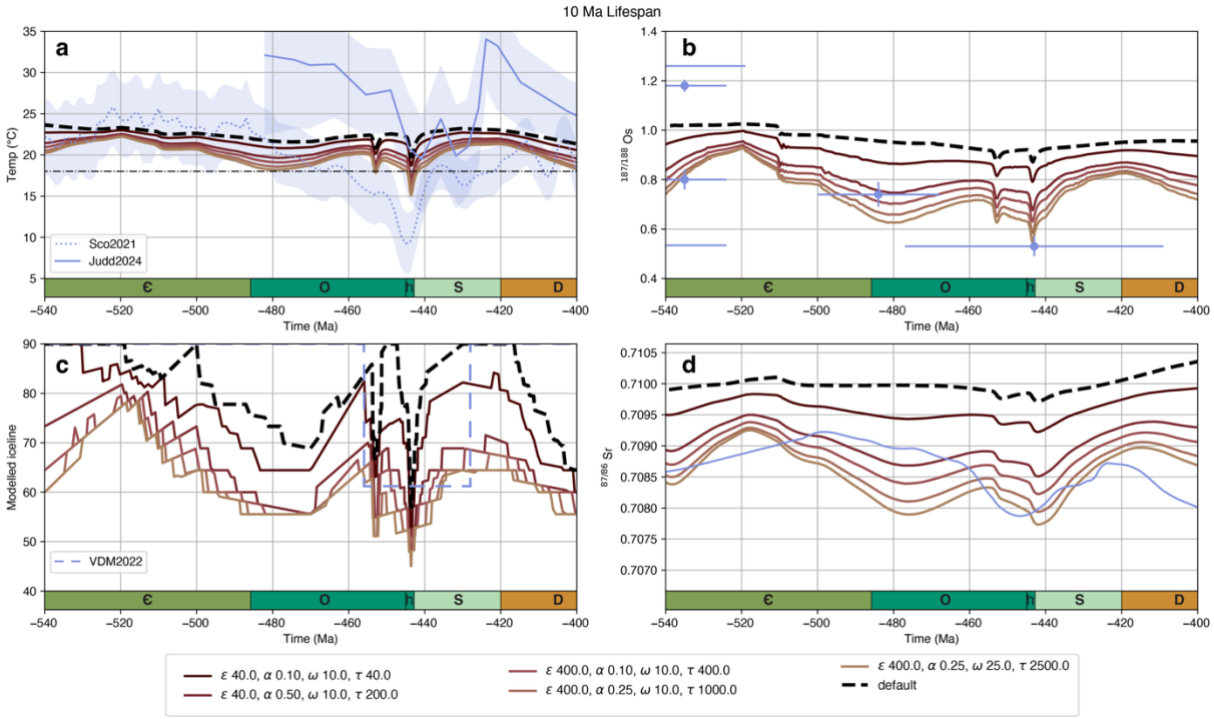

Figure 4: Preferred model results assuming a 10 Ma lifespan of ocean arc islands with proxy data. Default model run (i.e. no contribution from ocean arcs) is shown as the black dashed line in each respective panel. (a) global average surface temperature. (b) modelled $^{187/188}$Os of seawater. (c) modelled iceline results. (d) modelled $^{87/86}$Sr of seawater. Temperature proxies from Figure 1 are depicted in blue.